Journal of Power Sources 240 (2013) 404–410

Contents lists available at SciVerse ScienceDirect

Journal of Power Sources

journal homepage: www.elsevier.com/locate/jpowsour

Methanol generation by CO_2 reduction at a Pt–Ru/C electrocatalyst using a membrane electrode assembly

Sayoko Shironita [a], Ko Karasuda [a], Kazutaka Sato [a], Minoru Umeda [a,b,*]

[a] Department of Materials Science and Technology, Faculty of Engineering, Nagaoka University of Technology, 1603-1 Kamitomioka, Nagaoka, Niigata 940-2188, Japan
[b] JST, ACT-C, 4-1-8 Honcho, Kawaguchi, Saitama 332-0012, Japan

HIGHLIGHTS

- We compared the CO_2 electroreduction to generate methanol at Pt/C and Pt–Ru/C.
- CO_2 was electrochemically reduced using Pt–Ru/C MEA at 0.06–0.25 V vs. DHE.
- Methanol is detected as the main product of the CO_2 reduction.
- By using Pt–Ru/C, the methanol yield and coulombic efficiency were 7.5% and 75%, respectively.
- Pt–Ru/C has a higher efficiency than Pt/C, because Ru effectively acts during the CO_2 reduction.

ARTICLE INFO

Article history:
Received 31 January 2013
Received in revised form
5 April 2013
Accepted 7 April 2013
Available online 18 April 2013

Keywords:
Membrane electrode assembly
Carbon dioxide electroreduction
Pt–Ru/C
Methanol generation
Reversible fuel cell

ABSTRACT

We have investigated the CO_2 electroreduction at a Pt–Ru/C-based catalyst using a membrane electrode assembly (MEA) in a single cell to realize a methanol-based reversible fuel cell. Cyclic voltammograms were measured under N_2 and CO_2 atmospheres using the Pt–Ru/C-based MEA. For comparison, the Pt/C-based MEA was used. A typical voltammogram attributed to the Pt electrode has been obtained using Pt/C under an N_2 atmosphere, and an extra oxidation peak appeared at 0.60 V vs. DHE under a CO_2 atmosphere. This peak has been considered to be caused by the re-oxidation of the CO_2 reductant. For the Pt–Ru/C, the re-oxidation peak has been observed at 0.50 V vs. DHE which is more negative than Pt/C. The limiting cathode potential of the cyclic voltammogram was changed from 0.06 to 0.35 V vs. DHE under a CO_2 atmosphere, and the magnitude of the re-oxidation peak decreased. To quantitatively analyze the product of the CO_2 reduction, a gas chromatograph and methanol- and CO-stripping voltammograms were measured. Based on these results, methanol has been found to be the main product of the CO_2 reduction at the Pt–Ru/C. Finally, the methanol yield and coulombic efficiency were calculated resulting in 7.5% and 75% at the Pt–Ru/C, respectively.

1. Introduction

A reversible fuel cell (RFC) is an electrochemical device, in which electric energy is converted into chemical energy and vice versa. It functions as an energy storage device just like secondary batteries [1–5]. When one compares the two in terms of the energy storage capacity, that of the secondary battery is limited by the used quantity of the electrode active materials; while that of the RFC is determined by the tank volume for the chemical storage. In addition, the RFC never undergoes a self-discharge. These characteristics denote that the RFC is suitable for long-term energy storage and a high capacity.

As representatives of the RFCs, the H_2/O_2 type and acetone/isopropanol type are well known; although the latter is used as an energy converter from thermal energy to electrical energy [6–12]. With regard to the former H_2/O_2 type, it stores H_2 and O_2 generated by the H_2O electrolysis, thereafter utilizing them for power generation [6–10]. In that system, the H_2 and O_2 gases are required to be stored under high-pressure conditions. From the viewpoint of safety chemical storage, liquid alcohols are thought to be ideal chemicals, because they are stable under atmospheric pressure and room temperature.

As a representative of alcoholic fuel cells, a direct methanol fuel cell (DMFC) has been practically used in which a liquid methanol solution is fed to the anode for the power generation [13–16]. The anode and cathode reactions for the DMFC power generation are respectively represented as follows;

$$CH_3OH + H_2O \rightarrow CO_2 + 6H^+ + 6e^- \quad (1)$$

* Corresponding author. Department of Materials Science and Technology, Faculty of Engineering, Nagaoka University of Technology, 1603-1 Kamitomioka, Nagaoka, Niigata 940-2188, Japan. Tel./fax: +81 258 47 9323.
E-mail address: mumeda@vos.nagaokaut.ac.jp (M. Umeda).

0378-7753/$ – see front matter © 2013 Elsevier B.V. All rights reserved.
http://dx.doi.org/10.1016/j.jpowsour.2013.04.034

$$3/2O_2 + 6H^+ + 6e^- \rightarrow 3H_2O \quad (2)$$

The main product, CO_2, is chemically stable and is known to be scarcely reduced. When the CO_2 is reduced in aqueous electrolyte solutions, it needs a high overpotential of more than 1 V and the products are reported to be formic acid, methane, etc [17–27]. Based on these reports, it is believed that the methanol electrooxidation easily takes place to generate the CO_2, whereas the inverse reaction hardly occurs. It is worthwhile to investigate the inverse reaction of Eq. (1) for realizing the methanol-based reversible fuel cell utilizing the reversible reactions of Eqs. (1) and (2).

Recently, some reports have suggested that CO_2 reduction occurs in a polymer electrolyte fuel cell, but the products have not been clearly identified [24,25]. Previously, we reported the behavior of CO_2 electroreduction at a Pt/C-based electrocatalyst of a membrane electrode assembly (MEA) in a single cell [28]. The main product of the reaction was estimated to be methanol. Its coulombic efficiency was expected to be 40%, however, the exhausted methanol yield from the cell was $\approx 10^{-2}$%. This big difference can be explained in that almost all of the reductant adsorbs on the electrode surface so that it is hardly removed. If it is possible to weaken the adsorption force by changing the electrocatalyst, the product will be easily removed and provide a high efficiency. This consideration enables us to develop the methanol-based RFC.

In this report, we conducted the CO_2 electroreduction at a Pt–Ru/C-based MEA by comparing to that using the Pt/C, resulting in the CO_2 reduction that progressively occurs with a low overpotential. We first carried out the cyclic voltammogram measurement in a CO_2 atmosphere at the Pt–Ru/C. A Pt–C was used for comparison. Next, the product analysis of the exhaust gas was performed by a gas chromatograph. The CO- and methanol-stripping voltammograms were conducted to confirm the products. Finally, the methanol yield and coulombic efficiency were evaluated.

2. Experimental

2.1. Preparation of a single cell

Commercially available Pt/C (Pt: 45.7 wt%) and Pt–Ru/C (Pt: 32.6 wt%, Ru: 16.9 wt%) electrocatalyst powders were purchased from Tanaka Kikinzoku Kogyo Co., Ltd. At first, an MEA (geometric electrode area: 5 cm^2) having two Pt/Cs as the working and counter electrodes was prepared as follows [29–31]: Nafion 117 (5 × 5 cm, DuPont) was used as the polymer electrolyte membrane. The membrane was boiled in a 0.5 mol dm^{-3} H_2SO_4 solution, and then washed twice by boiling in distilled water for 1 h. Two to three drops of Milli-Q water were added to the Pt/C powder and mixed using a ball mill for 5 min, after which the mixtures were diluted by a mixed solvent of methanol, 2-propanol, and Milli-Q water (weight ratio was 1:1:1). Next, a 5 wt% Nafion 117 solution was added to the diluted mixtures so that the weight ratio was 1:6 (Nafion:Pt/C powder), and dispersed using a ball mill for one day. The obtained catalyst slurry was sprayed over a piece of water-repellent carbon paper (2.3 × 2.3 cm, TGP-H060, Toray Industries, Inc.), such that the amount of metal was 1.0 mg cm^{-2}. Subsequently, the pretreated Nafion 117 membrane was sandwiched between the two pieces of Pt/C-coated carbon paper and hot-pressed at 4.5 kN and 140 °C for 10 min.

Another type of MEA was prepared using Pt–Ru/C and Pt/C as the working and counter electrodes, respectively. The slurry of Pt–Ru/C was prepared in the same manner as mentioned above and sprayed over the carbon paper. The pretreated Nafion 117 membrane was then sandwiched between the Pt–Ru/C-coated carbon paper and Pt/C-coated one, and hot-pressed under the same conditions. We used two types of MEAs in this study. Each prepared MEA was installed in a single cell (ElectroChem, Inc., E3156) having a dynamic hydrogen electrode (DHE) as the reference electrode. A schematic of the single cell and experimental apparatus is shown in Fig. 1.

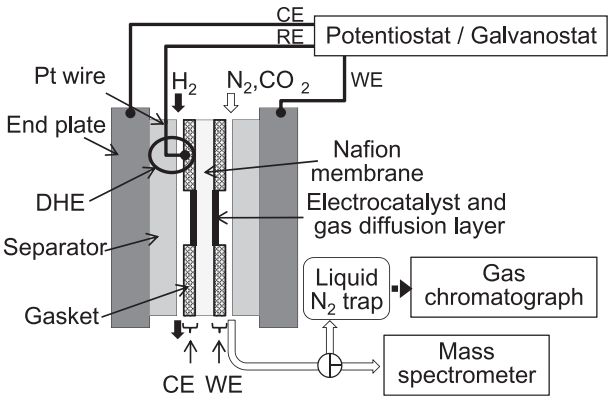

Fig. 1. Schematic of a single cell equipped with DHE reference electrode and experimental apparatus.

2.2. Electrochemical measurements

The temperature of the MEA-installed cell was controlled at 40 °C unless otherwise mentioned. Humidified N_2 (purity: 99.999%) and humidified H_2 (purity: 99.999%) were supplied to the working and counter electrodes, respectively, at the flow rate of 50 cm^3 min^{-1} by a PEFC power generation unit (HPE-1000, FC Development Co., Ltd.) [32]. H_2 was supplied to the counter electrode, so that the electrode reaction will not be the rate determining step. Under these conditions, the electrode potential was swept at a rate of 50 mV s^{-1}. The potential range of the observed voltammogram was stabilized at 0.06–1.40 V vs. DHE for the Pt/C-based electrode. For the Pt–Ru/C working electrode, the potential range was 0.06–0.70 V vs. DHE because Ru will dissolve at >0.70 V vs. DHE. Next, the gas supplied for the working electrode was changed from humidified N_2 to humidified CO_2 (purity: 99.995%), and the cyclic voltammogram was then measured at the rate of 10 mV s^{-1} in the potential range. All gases in this study were fully humidified at all the subsequent cell temperatures for the measurements.

2.3. Analyses of products

Methanol-stripping voltammetry was performed as follows: The Pt–Ru/C working electrode potential was fixed at 0.10 V vs. DHE; N_2 gas then bubbled into a bottle of liquid methanol at 50 cm^3 min^{-1} (Purity: 99.95%, Wako) and humidified H_2 at 50 cm^3 min^{-1} were supplied to the working and counter electrodes, respectively, for 10 min. Thereafter, 50 cm^3 min^{-1} humidified N_2 was supplied to the working electrode for 1 h, while the electrode potential was maintained at 0.10 V vs. DHE. The 2-cycle voltammogram was obtained between potential voltages of 0.06–0.70 V vs. DHE with a sweep rate of 10 mV s^{-1}.

A CO-stripping voltammetry was conducted as follows: Similar to the methanol-stripping measurement, the working electrode potential was fixed at 0.10 V vs. DHE, and humidified CO at 10 cm^3 min^{-1} and humidified H_2 at 50 cm^3 min^{-1} were supplied to the working and counter electrodes, respectively, for 10 min. Subsequently, humidified N_2 was supplied to the working electrode for

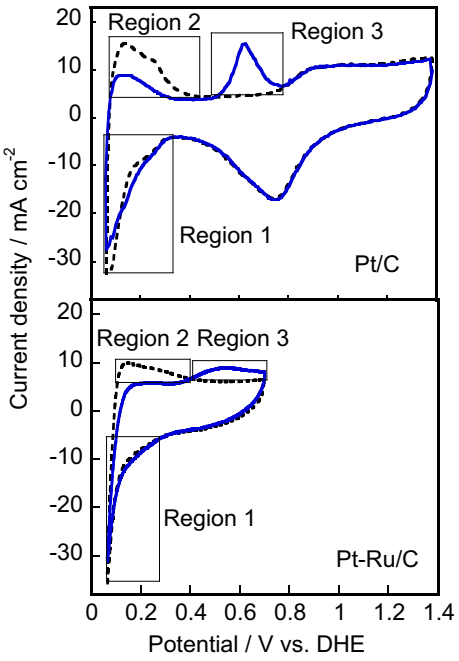

Fig. 2. Cyclic voltammograms obtained at Pt/C (upper) and Pt–Ru/C (lower) under CO_2 (solid lines) and N_2 (dotted lines) atmospheres at 40 °C. Sweep rate: 10 mV s^{-1}.

1 h at 50 cm^3 min^{-1}, while the electrode potential was maintained at 0.10 V vs. DHE. The voltammogram was then measured using the same procedure for the methanol-stripping measurement.

To analyze the products of the reaction, the cell cathode was operated by supplying humidified CO_2 to the working electrode and humidified H_2 to the counter electrode for 5 h at 0.06 V vs. DHE at 80 °C. During the operation, the exhaust gas from the working electrode was trapped by liquid N_2 and then injected into a gas chromatograph (6890 series gas chromatograph, Agilent Technology, Inc.) as shown in Fig. 1. The capillary column used was a high polarity polyethylene glycol column (DB-WX123-7033, Agilent Technology, Inc.), with helium gas used at 3.0 cm^3 min^{-1} as the carrier gas. A hydrogen flame ionization detector was used for the measurements.

Moreover, the exhaust gas from the working electrode was directly introduced to a quadrupole mass spectrometer (QME200, PFEIFFER) as seen in Fig. 1. The cell temperature was 80 °C and the working electrode potential was 0.06 V vs. DHE. Humidified CO_2 and humidified H_2 were supplied to the working and counter electrodes, respectively, at the flow rate of 50 cm^3 min^{-1}.

3. Results and discussion

3.1. Cyclic voltammograms of Pt–Ru/C under a CO_2 atmosphere

To investigate the electrochemical CO_2 reduction reaction at the Pt–Ru/C, cyclic voltammograms were measured using the Pt–Ru/C-based MEA in a single cell equipped with a reference electrode (DHE). Also, the Pt/C-based MEA was used for comparison. The voltammograms of the Pt/C and Pt–Ru/C under CO_2 are shown as solid lines in Fig. 2. As background voltammograms, the voltammograms under a N_2 atmosphere are presented in the same figure as dotted lines. All the voltammograms of Fig. 2 are obtained from the fifth cycle of the successive potential sweeps, which ensures that the CVs are measured under a steady state condition.

In upper figure for the Pt/C, a typical cyclic voltammogram of Pt is observed under the N_2 atmosphere, representing characteristics such as the H–adsorption/desorption at 0.06–0.40 V vs. DHE, the formation of an oxide layer on the Pt surface at 0.80–1.40 V vs. DHE, and the reduction of the Pt oxide layer at around 0.70 V vs. DHE [33]. In the CO_2 atmosphere, three characteristic peaks are observed and designated as Region 1, Region 2, and Region 3.

In Region 1 of the upper Fig. 2, the reduction current under the CO_2 atmosphere is as high as that under the N_2 atmosphere. In Region 2, the H–desorption region, the oxidation current under the CO_2 atmosphere is lower than that under the N_2 atmosphere. This implies that the desorption amount of adsorbed H on the Pt surface under the CO_2 atmosphere is smaller than that under the N_2 one. From the view point of a coulombic balance, this result is inconsistent with the observation in Region 1. In Region 3, a new current peak is observed under the CO_2 atmosphere, although there is no peak under the N_2 atmosphere. Based on these results, it is deduced that the CO_2 reduction occurs in Region 1, which competes with the H–adsorption reaction, and the CO_2 reduction product or intermediate is reoxidized in Region 3.

For the Pt–Ru/C, the three peaks are also observed in Fig. 2 lower. By comparing the peaks of Regions 1–3 at the Pt/C and Pt–Ru/C, the peaks of Regions 1and 2 have almost the same tendency. There is no difference between the N_2 and CO_2 atmospheres in Region 1, and the oxidation current from the H–desorption in Region 2 decreases by changing the gas from N_2 to CO_2 in the same potential region for the Pt/C. However, in Region 3, the re-oxidation of the CO_2 reductant at the Pt–Ru/C occurs at a more negative potential than that at the Pt/C. It is noteworthy that the electrochemically CO_2 reduction at the Pt–Ru/C catalyst has never been reported before.

3.2. Electrochemical evaluation of CO_2 electroreduction

According to the aforementioned deduction, we can presume that the oxidation peak in Region 3 of Fig. 2 indicates the re-oxidation of the CO_2 reductant. Based on this hypothesis, a linear sweep voltammogram was then measured by changing the initial holding potential. The results are shown in Fig. 3. The initial holding potential was gradually changed from 0.06 to 0.35 V vs. DHE. Each holding time was 5 min by supplying humidified CO_2 at 50 cm^3 min^{-1}. The electrode potential was then swept between the initial holding potential and 0.70 V vs. DHE for two cycles (0.06–0.70 V vs. DHE, 10 mV s^{-1}). The second cycle CV in the upper left figure of Fig. 3 was obtained under the same condition as the solid line seen in the lower figure of Fig. 2.

In Fig. 3, the solid and broken lines denote the first and second potential cycles, respectively. As for the first cycle, the magnitude of the peak current during the first sweep that appeared in Region 3 gradually decreased with the increasing initial holding potential. Also, the peak during the second cycle in Region 3 gradually decreased with the increasing initial holding potential.

The relationship between the coulombic charge in Region 3 in the first sweep voltammogram (Fig. 3) vs. the initial holding potential is plotted in Fig. 4 and denoted by the triangular symbols. The magnitude of this charge is observed to decrease with a shift in the holding potential from 0.10 V vs. DHE in the anodic direction, while it is almost the same at 0.10–0.06 V vs. DHE. It is considered that the CO_2 electroreduction occurs at 0.06–0.25 V vs. DHE and its reductant is adsorbed on the electrode surface or exists adjacent to the electrode.

Next, the coulombic charge in Region 3 in the second sweep voltammogram of the successive potential sweep is taken from Fig. 3 and plotted vs. the cathode limiting potential in Fig. 4 and denoted by the circular symbols. As in the case of the coulombic charge of the first sweep, the magnitude decreases with the increasing cathode limiting potential. The coulombic charge

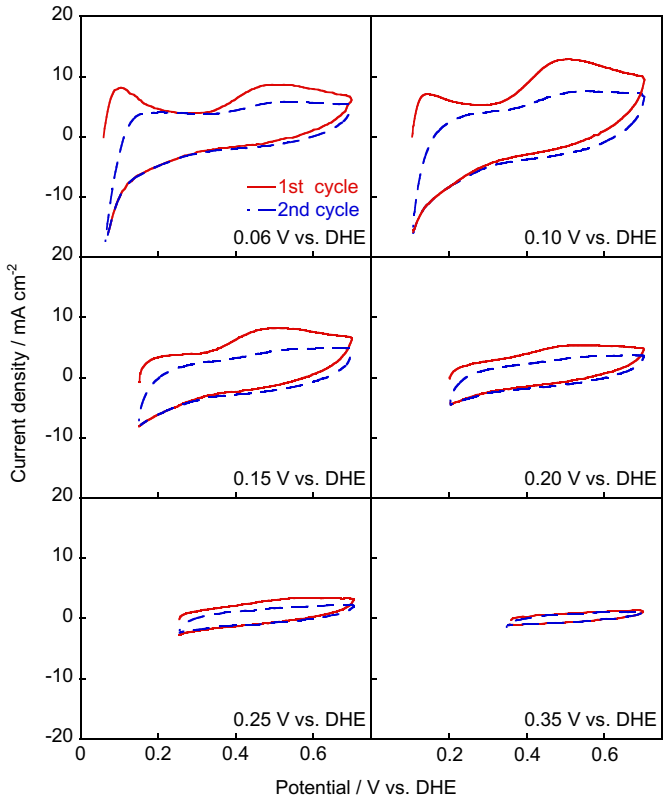

Fig. 3. The 2-cycle voltammograms obtained under CO_2 after the 5-min potential holding at Pt–Ru/C and 40 °C. The holding potential was changed from 0.06 to 0.35 V vs. DHE.

magnitude of the triangular plots is greater than that of the circular labeled plots, because the holding time of the first sweep is longer than that of the second successive sweep.

3.3. Product analysis of the CO_2 electroreduction

The methanol stripping voltammetry measurements were conducted to confirm the CO_2 electroreduction product at the Pt–Ru/C. The result is shown in Fig. 5a. In this figure, the methanol oxidation occurs at 0.50 V vs. DHE and its onset potential is 0.35 V

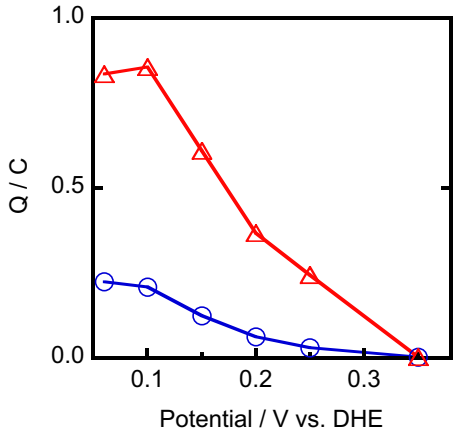

Fig. 4. Coulomb charges (Q) for the CO_2 re-oxidation peak vs. the initial holding potential (triangle). The initial holding time was 5 min. Plots of Q measured under successive potential sweeps are shown (circle).

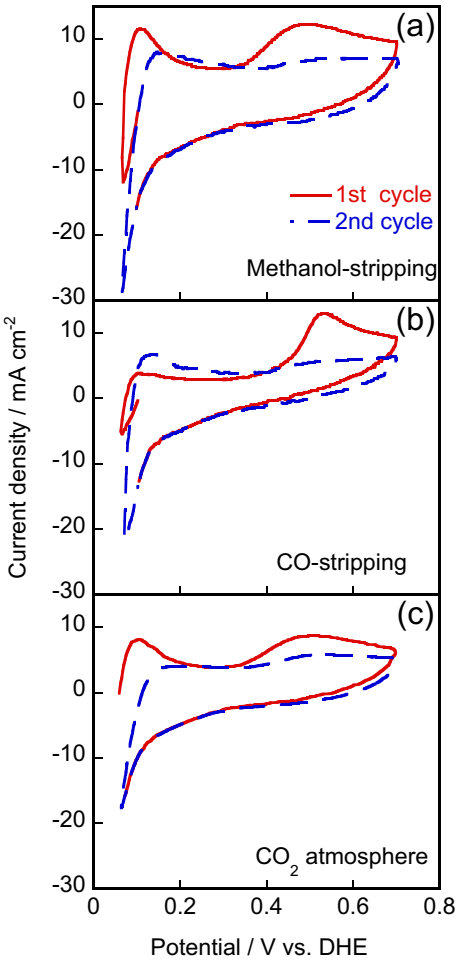

Fig. 5. (a) Methanol-stripping and (b) CO-stripping voltammograms at Pt–Ru/C-based MEA at 40 °C. (c) Lower graph is taken under CO_2 atmosphere for comparison at 40 °C. Sweep rate: 10 mV s^{-1}.

vs. DHE. These potentials are almost identical to the voltammogram under the CO_2 atmosphere (Fig. 5c), in which the re-oxidation onset potential is at 0.35 V vs. DHE and the peak is located approximately at 0.50 V vs. DHE.

According to previous reports, CO is considered to be generated as a product of the CO_2 electroreduction [18–23,26]. In this experiment using Pt–Ru/C, the CO-stripping voltammogram was measured. The result is shown in Fig. 5b. It was found that CO is completely desorbed by oxidation during the first cycle, since the voltammogram of the second cycle was almost identical to the shape that was obtained under the N_2 atmosphere (see Fig. 2). This result shows that the CO oxidation began from 0.40 V vs. DHE on the Pt–Ru/C, and an oxidation peak is observed at 0.53 V vs. DHE.

Next, the results of the methanol- and CO-stripping voltammograms are compared. For the methanol-stripping, an anodic current is observed at around 0.10 V vs. DHE in the first sweep voltammogram of Fig. 5a. This current peak is believed to be based on the methanol dissociative adsorption at the Pt–Ru/C catalyst [34,35]. On the other hand, there is no anodic peak around at 0.10 V vs. DHE in the CO-stripping voltammogram in Fig. 5b, because CO does not contain an H atom. Hence, the dissociative adsorption is hardly observed in the CO-stripping voltammogram. The voltammogram shape of Fig. 5c is similar not to Fig. 5b, but to Fig. 5a. Therefore, it is presumed that the product is methanol.

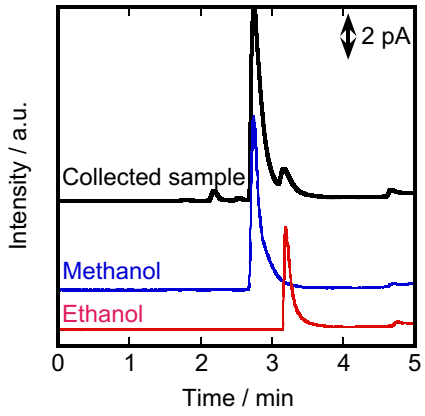

Fig. 6. Gas chromatograph of the cathode exhausted liquid from the single cell under CO_2 reduction operated at 0.06 V vs. DHE and 80 °C for 5 h. As references, 1 mmol dm^{-3} methanol and 1 mmol dm^{-3} ethanol are shown.

Having established that the CO_2 reduction reaction occurs at the Pt–Ru/C catalyst, we then investigated the products of the CO_2 reduction in the single cell. After a 5-h operation of the MEA at 0.06 V vs. DHE and at 80 °C, the exhausted gas was trapped using liquid N_2 and analyzed by gas chromatography. The resulting gas chromatograph is shown in Fig. 6, in which methanol and ethanol are used as references. As a result, methanol and a very small amount of ethanol were detected as reduction products. Mass spectrometry detected the peaks of m/z = 29, 31, and 32 in the exhausted gas. Therefore, the main product was confirmed to be methanol.

3.4. Electrode potential of CO_2 reduction

Based on the results described in the last section, methanol and a small amount of ethanol were detected by the gas chromatograph. From Figs. 3 and 4, the CO_2 electroreduction is known to predominantly occur at 0.06–0.25 V vs. DHE. These potentials are more positive than 0.016 V vs. NHE and 0.084 V vs. NHE, which are the standard electrode potential of methanol and ethanol [36]. The DHE potential using Nafion 117 is approximately the same as that of a normal hydrogen electrode (NHE) [37,38].

$$CO_2 + 6H^+ + 6e^- = CH_3OH + H_2O,\ E^o = 0.016\ V \quad (3)$$

$$2CO_2 + 12H^+ + 12e^- = C_2H_5OH + 3H_2O,\ E^o = 0.084\ V \quad (4)$$

When one considers the concentration dependence of the equilibrium potential, it can be calculated by the Nernst equation using the methanol activity of $1–1 \times 10^{-4}$, which is commonly employed in a theoretical estimation [39]. From the experimental condition, the partial pressure of CO_2 is 1 at 40 °C. These lead to the equilibrium potential of 0.016–0.057 V vs. NHE. As for ethanol, it is also estimated to be 0.084–0.105 V vs. NHE. Based on these results, the equilibrium electrode potential of the CO_2 reduction to generate alcohols is known to be 0.016–0.105 V vs. NHE.

In general, no current is observed for the coupled reversible reactions at the standard electrode potential because of the balanced anodic and cathodic currents. When we look at the reduction reaction, it proceeds even when the potential is more positive than the standard electrode potential [40]. However, this small reduction current is unable to be observed due to the relatively large coupled oxidation current.

The methanol oxidation reaction (MOR), which is a coupled reaction of the CO_2 reduction, accompanies the formation of CO and other intermediates that strongly adsorb on the electrocatalyst surface [41]. For this reason, the onset potential of the MOR shifts in the positive direction and is observed at 0.35 V vs. NHE as shown in Fig. 5. As a result of this anodic potential shift of the coupled MOR, it could be considered that the CO_2 reduction is observed at 0.06–0.25 V vs. DHE, as seen in Fig. 4, which is a substantially more positive potential than the equilibrium electrode potentials of 0.016–0.057 V vs. NHE and 0.084–0.105 V vs. NHE.

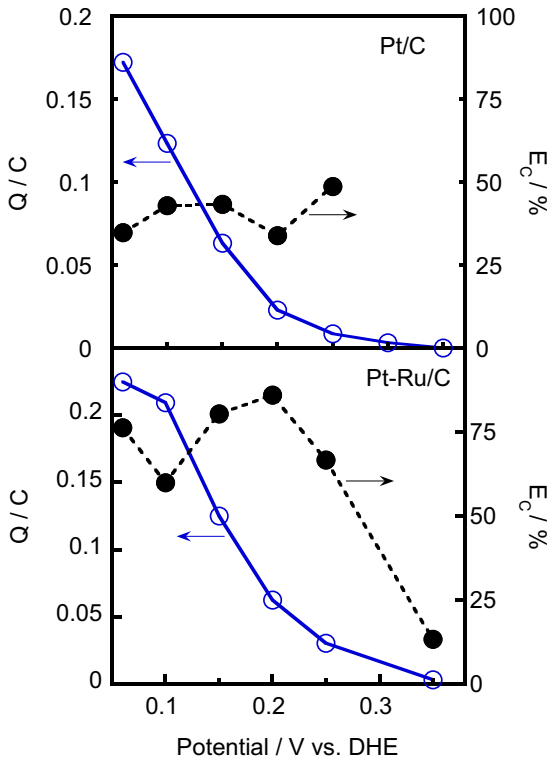

Fig. 7. Coulomb charges (Q) of the oxidation peak that appeared at Pt/C and Pt–Ru/C in CO_2 atmosphere (○), and the coulombic efficiency (E_c) of CO_2 reductant (intermediate) defined by Eq. (1) (●).

It should be noted that the CO_2 reduction proceeds with a low overpotential at the Pt–Ru/C of the MEA in this experiment. Under these conditions, the hydrogen evolution reaction as a competition reaction is low because the CO_2 reduction potential is more positive than that of $2H^+ + 2e^- = H_2$ (E^o = 0.000 V vs. NHE). Therefore, the CO_2 reduction predominantly occurred at the Pt–Ru/C MEA.

3.5. Coulombic efficiency of the CO_2 reduction

The reduction current observed at Region 1 in Fig. 2 is postulated to be the reactions of (i) the CO_2 reduction and (ii) the H–adsorption that simultaneously occur on the electrode. The coulombic efficiency of the former reaction is carried out by calculating the ratio from the CO_2 reductant (E_c) using the coulombic charges of Region 1 (Q1) and Region 3 (Q3) as shown in Fig. 3. The ratio is calculated using Eq. (5).

$$E_c = Q3/Q1 \times 100 \quad (5)$$

where Q3 represents the anodic charges of Region 3 caused by the reoxidation of the CO_2 reductant, and Q1 represents the total cathodic charges incorporating the CO_2 reduction and the H–adsorption on the electrode observed in Region 1.

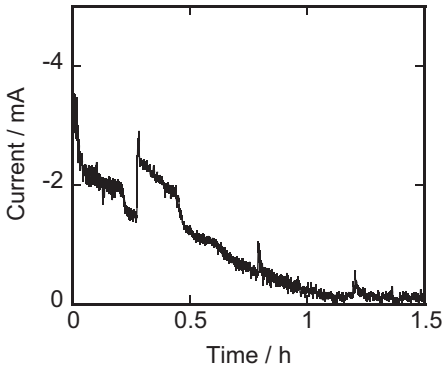

Fig. 8. Chronoamperogram at Pt–Ru/C under CO_2 atmosphere. Cell temperature: 40 °C, working electrode potential: 0.06 V vs. DHE.

For this evaluation, the cyclic voltammograms in Fig. 2 were used. The coulombic efficiencies, E_c, are calculated and plotted vs. the lower potential limit of the cyclic voltammograms in Fig. 7. In this figure, the coulombic efficiencies are indicated by the closed circle (E_c). An open circle shows the charge (Q3) caused by the re-oxidation of the CO_2 reduction in Region 3. The results show that the coulombic efficiency of the CO_2 reduction ranged between 30 and 50% at 0.06–0.25 V vs. DHE in the case of the Pt/C. On the other hand, the efficiency was 60–80% at 0.06–0.25 V vs. DHE for the Pt–Ru/C. Although, there is no significant difference in the coulombic charge of re-oxidation between the Pt/C and Pt–Ru/C, the coulombic efficiency is significantly enhanced by the addition of Ru. It is reported that the methanol electrooxidation pathway is considered as follows [42]:

$$Pt + CH_3OH \rightarrow Pt(CH_3OH)_{ads} \quad (6)$$

$$Pt(CH_3OH)_{ads} \rightarrow Pt(CH_{4-n}O) + nH^+ + ne^- \quad (7)$$

$$M + H_2O \rightarrow M\text{-}OH + H^+ + e^- \quad (8)$$

$$Pt{-}CO + M\text{-}OH \rightarrow CO_2 + H^+ + e^- \quad (9)$$

$$Pt{-}CO + H_2O \rightarrow CO_2 + 2H^+ + 2e^- \quad (10)$$

By an addition of Ru, the formation of Pt–CO and Ru–OH from CO_2 during its electroreduction, i.e., the reverse reaction of Eq. (9), probably takes place. Therefore, the coulombic efficiency, E_R, is improved at the Pt–Ru/C by the Ru addition.

Next, chronoamperometry was conducted at 0.06 V vs. DHE and 80 °C by supplying the humidified CO_2 and humidified H_2 to the working and counter electrodes, respectively, for 1.5 h. The electrode potential was set at 0.06 V vs. DHE which is the same as that of gas chromatograph measurement. At that potential, the CO_2 reduction and H–adsorption reactions take place on the electrode. The result is shown in Fig. 8, which demonstrates the continuous reduction of CO_2. However, the magnitude of the current is observed to decrease with the increasing electrolysis time. The result of the methanol-stripping voltammogram as mentioned above showed that methanol strongly adsorbs on the electrocatalyst surface. The results observed in Fig. 8 can therefore be explained by the increasing accumulation of methanol on the electrocatalyst surface, which consequently results in a decrease in the number of active sites on the electrocatalyst.

In Fig. 7, the coulombic efficiencies of the CO_2 reduction are approximately 35% at the Pt/C and 76% at the Pt–Ru/C at 0.06 V vs. DHE. However, as shown in Fig. 8, the reduction current decreased with an increase in the electrolysis time. The difference observed between these two results can be explained by the fact that the electrolysis was conducted for a short period of time in the former case (Fig. 7) and for a longer period of time in the latter one (Fig. 8). The methanol yields detected in the exhaust gas were ≈0.03% and 7.5% at the Pt/C and Pt–Ru/C, respectively (Table 1). However, our analysis showed distinct evidence that the CO_2 reduction proceeds with the high coulombic efficiency of 35% and 76% based on the electrochemical assessment in the cell at the Pt/C and Pt–Ru/C, respectively. Accordingly, it is most likely that almost all of the CO_2 reductant is strongly adsorbed on the Pt surface. If these adsorbates can be efficiently removed from the electrode surface, we can expect that the CO_2 reduction can continuously occur without any decrease in the reduction current attributed to the catalyst poisoning.

Table 1
Comparison of methanol yield at Pt/C and Pt–Ru/C at 0.06 V vs. DHE and 80 °C.

	Pt/C	Pt–Ru/C
Coulombic efficiency	35%	75%
Methanol yield	≈0.03%	7.5%

4. Conclusions

The electrochemical CO_2 reduction was investigated using an MEA with a Pt–Ru/C electrocatalyst under a CO_2 gas atmosphere in a single cell. A summary of the results is as follows:

(1) A cyclic voltammogram was obtained under a CO_2 atmosphere, and the re-oxidation peak of the CO_2 reductant was observed at 0.60 V vs. DHE and Pt/C. The peak of Pt–Ru/C was located at 0.50 V vs. DHE and it suggested that the CO_2 reduction certainly occurs at the Pt–Ru/C catalyst.
(2) By changing the CO_2 reduction holding potential of the cyclic voltammetry, the magnitude of the re-oxidation peak decreased when the holding potential shifted from 0.06 to 0.35 V vs. DHE.
(3) From the methanol- and CO-stripping voltammograms and the gas chromatograph measurements of the exhaust gas from a single cell, it was confirmed that methanol is produced at the Pt–Ru/C MEA during the CO_2 electroreduction.
(4) The methanol yield efficiency was improved from 0.03% at the Pt/C to 7.5% at the Pt–Ru/C. The evaluated coulombic efficiencies by cyclic voltammetry measurements were 35% and 75% at the Pt/C and Pt–Ru/C, respectively.

Acknowledgment

A part of this work was supported by MEXT/JSPS KAKENHI, grant number 24350091.

References

[1] A.B. LaConti, L. Swette, in: W. Vielstich, A. Lamm, H.A. Gasteiger (Eds.), Handbook of Fuel Cells, vol. 4, John Wiley and Sons, Ltd., England, 2003, pp. 745–761.
[2] T. Ioroi, T. Oku, K. Yasuda, N. Kumagai, Y. Miyazaki, J. Power Sources 124 (2003) 385–389.
[3] S.A. Grigoriev, P. Millet, V.I. Porembsky, V.N. Fateev, Int. J. Hydrogen Energy 36 (2011) 4164–4168.
[4] P. Millet, R. Ngameni, S.A. Grigoriev, V.N. Fateev, Int. J. Hydrogen Energy 36 (2011) 4156–4163.
[5] C.M. Hwang, M. Ishida, H. Ito, T. Maeda, A. Nakano, A. Kato, T. Yoshida, J. Power Sources 202 (2012) 108–113.
[6] C.C. Badcock, Aerosp. Am. 22 (1984) 68–72.
[7] D.W. Sheibley, NASA Conf. Publ. (1984) 23–38.

[8] G.M. Reppucci, A.A. Sorensen, Intersoc. Energy Convers. Eng. Conf. 20 (1985) 66–73.
[9] A.J. Appleby, J. Power Sources 22 (1988) 377–385.
[10] J. Giner, A. LaConti, in: V. Barsukov, F. Beck (Eds.), New Promising Electrochemical Systems for Rechargeable Batteries, Kluwer Academic Publishers, Dordrecht, 1996, pp. 215–232.
[11] Y. Ando, T. Tanaka, T. Doi, T. Takashima, Energy Convers. Manage. 42 (2001) 1807–1816.
[12] Y. Ando, Y. Aoyama, T. Sasaki, Y. Saito, H. Hatori, T. Tanaka, Bull. Chem. Soc. Jpn. 77 (2004) 1855–1859.
[13] R. Dillon, S. Srinivasan, A.S. Aricò, V. Antonucci, in: N. Brandon, D. Thompsett (Eds.), Fuel Cells Compendium, Elsevier, Amsterdam, Netherlands, 2005, pp. 167–187.
[14] D.C. Dunwoody, H. Chung, L. Haverhals, J. Leddy, in: S. Minteer (Ed.), Alcoholic Fuels, Taylor & Francis, 2006, pp. 155–189. FL.
[15] S. Prakash, W.E. Mustain, P.A. Kohl, in: T.S. Zhao (Ed.), Micro Fuel Cells: Principles and Applications, Elsevier, Amsterdam, Netherlands, 2009, pp. 1–50.
[16] J. Kawaji, S. Suzuki, Y. Takamori, M. Morishima, Electrochim. Acta 55 (2010) 8018–8022.
[17] P.G. Russell, N. Kovac, S. Srinivasan, M. Steinberg, J. Electrochem. Soc. 124 (1977) 1329–1338.
[18] M. Watanabe, M. Shibata, A. Katoh, J. Electroanal. Chem. 305 (1991) 319–328.
[19] G. Kyriacou, A. Anagnostopoulos, J. Electroanal. Chem. 322 (1992) 233–246.
[20] Y. Hori, H. Wakebe, T. Tsukamoto, O. Koga, Electrochim. Acta 39 (1994) 1833–1839.
[21] T. Yamamoto, D.A. Tryk, A. Fujishima, H. Ohta, Electrochim. Acta 47 (2002) 3327–3334.
[22] Y. Hori, I. Takahashi, O. Koga, N. Hoshi, J. Phys. Chem. B 106 (2002) 15–17.
[23] I. Takahashi, O. Koga, N. Hoshi, Y. Hori, J. Electroanal. Chem. 533 (2002) 135–143.
[24] J. Liu, H. Yan, K. Wang, E. Wang, J. Appl. Electrochem. 34 (2004) 757–762.
[25] T. Smolinka, M. Heinen, Y.X. Chen, Z. Jusys, W. Lehnert, R.J. Behm, Electrochim. Acta 50 (2005) 5189–5199.
[26] M. Gattrell, N. Gupta, A. Co, Energy Convers. Manage. 48 (2007) 1255–1265.
[27] J. Christophe, T. Doneux, C. Buess-Herman, Electrocatalysis 3 (2012) 139–146.
[28] S. Shironita, K. Karasuda, M. Sato, M. Umeda, J. Power Sources 228 (2013) 68–74.
[29] M. Inoue, T. Iwasaki, K. Sayama, M. Umeda, J. Power Sources 195 (2010) 5986–5989.
[30] M. Umeda, K. Sayama, M. Inoue, J. Renewable Sustainable Energy 3 (2011) 043107.
[31] M. Inoue, T. Iwasaki, M. Umeda, Electrochemistry 79 (2011) 329–333.
[32] M. Umeda, S. Kawaguchi, I. Uchida, Jpn. J. Appl. Phys. 45 (2006) 6049–6054.
[33] B.E. Conway, H. Angerstein-Kozlowska, W.B.A. Sharp, E.E. Criddle, Anal. Chem. 45 (1973) 1331–1336.
[34] T. Iwasita, Electrochim. Acta 47 (2002) 3663–3674.
[35] K. Kashima, M. Umeda, A. Yamada, I. Uchida, Electrochemistry 74 (2006) 166–168.
[36] C. Lamy, A. Lima, V. LeRhun, F. Delime, C. Coutanceau, J.-M. Léger, J. Power Sources 105 (2002) 283–296.
[37] B. Seger, K. Vinodgopal, P.V. Kamat, Langmuir 23 (2007) 5471–5476.
[38] M. Umeda, K. Sayama, T. Maruta, M. Inoue, Ionics 19 (2013) 623–627.
[39] M. Pourbaix, in: J.A. Franklin (Tr.), Atlas of Electrochemical Equilibria in Aqueous Solutions, NACE, Houston, 1974.
[40] C.H. Hamann, A. Hamnett, W. Vielstich, Electrochemistry, second ed., WILEY-VCH Verlag GmbH & Co. KGaA, Weinheim, 2007, pp. pp.166–169.
[41] A. Hamnett, in: W. Vielstich, A. Lamm, H.A. Gasteiger (Eds.), Handbook of Fuel Cells, vol. 1, John Wiley and Sons, Ltd., England, 2003, pp. 305–322.
[42] M. Umeda, H. Sugii, I. Uchida, J. Power Sources 179 (2008) 489–496.